

Fano effect of metamaterial resonance in terahertz extraordinary transmission

Xiao Xiao,¹ Jinbo Wu,² Fumiaki Miyamaru,^{3,4} Mengying Zhang,² Shunbo Li,¹ Mitsuo W. Takeda,³ Weijia Wen,^{1,2,a)} and Ping Sheng^{1,2}

¹Department of Physics, The Hong Kong University of Science and Technology, Clear Water Bay, Kowloon, Hong Kong

²Nano Science and Nano Technology Program, The Hong Kong University of Science and Technology, Clear Water Bay, Kowloon, Hong Kong

³Department of Physics, Faculty of Science, Shinshu University, Matsumoto 390-8621, Japan

⁴PRESTO, Japan Science and Technology Agency, Aoba, Sendai 980-8577, Japan

(Received 10 November 2010; accepted 22 December 2010; published online 5 January 2011)

We show that the terahertz resonant transmission through metal hole array can be tailored by filling the holes with metamaterials. Experiment and finite difference time domain simulations show this type of resonant transmission to be induced by locally resonant modes, instead of the usual lateral surface grating mode. As the metamaterial's local resonances can be manipulated by varying their geometric configurations, this type of resonant transmission can be tuned over a broad frequency regime that is subwavelength to the array periodicity, with a transmission profile that can also be tailored by the frequency location of the resonance. Such tunability of resonant transmission, with its attendant enhanced local field intensity in the vicinity of the aperture, may provide some potential applications. © 2011 American Institute of Physics. [doi:10.1063/1.3541652]

Discovery of extraordinary transmission (ET) (Ref. 1) has opened the door to a great variety of potential applications.^{2–8} An important characteristic of the resonant transmission—the large field enhancement around the aperture regions—makes it an idea tool for biosensing^{9,10} and optical manipulations.¹¹ However, the resonant frequency of ET is closely related to the periodicity of the aperture array. It would be desirable if there can be additional channels for tuning the resonant transmission frequency, together with further increases in the near-field intensity.

In this work we report a type of resonant transmission induced by local resonances instead of surface grating modes. To achieve this effect, patterned metamaterial (MM) patches¹² were filled into the hole array to introduce local resonances. The new resonant transmission peak(s) appear at a much lower frequency than that of hole array. The resonant transmission can be well understood within the framework of Fano resonant scattering:^{13–15} the resonance induced by filled MM patches in hole array serves as Fano bound state, while the continuum scattering background (in the absence of the MM patches) plays the role of nonresonant channel, in conjunction with the Fabry–Perot (FP) resonances of the substrate.¹⁶ The wavelength at the resonant transmission frequency can be up to 100 times larger than the largest gaps in the hole region, and the attendant near-field enhancement can be up to five times larger than that in the metal hole array. The easy manipulation of metamaterial patches' resonances also offers a ready approach to tune the resonant transmission frequency as well as its transmission profile.

The sample studied is shown schematically in Fig. 1(a) and the optical image of the sample is shown in Fig. 1(b). A simple square lattice of square holes (each side 180 μm) was perforated in 0.4 μm thick gold film (on a 500 μm

thick silicon substrate), with a lattice constant of 300 μm . The MM patches preserve fourfold rotational symmetry [see Fig. 1(a)], and thus the incident polarization along the x direction makes no difference from that along the y direction. The transmission spectra were measured by terahertz time domain spectroscopy.¹⁷ The measured transmission spectrum of the sample is shown as the blue curve in Fig. 1(c) with comparison of that of the metal hole array (the red curve). Besides a common peak at 0.123 THz caused by FP resonances,¹⁶ we observed another transmission peak, about three times the height of the FP resonance peak, appearing at 0.161 THz, which is much lower than Wood's anomaly frequency of metal hole array at about 0.29 THz.

To understand the mechanism of the additional peak, finite difference time domain simulations¹⁸ were then performed with periodic boundary condition for both the sample shown in Fig. 1 and bare MM array of the same periodicity. From simulated results shown in Fig. 2, the resonance trans-

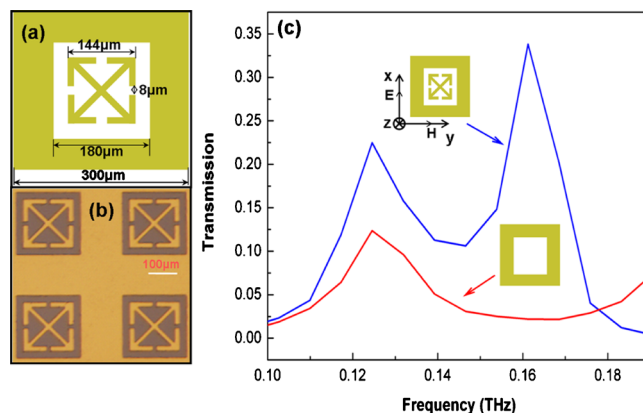


FIG. 1. (Color online) (a) Schematic illustration of the sample geometry showing the dimensions of the MM patches in the hole array. (b) An optical image of the actual sample. (c) Experimental transmission spectra for both the hole array with (upper curve) and without (lower curve) the MM fillings.

^{a)}Author to whom correspondence should be addressed. Electronic mail: phwen@ust.hk.

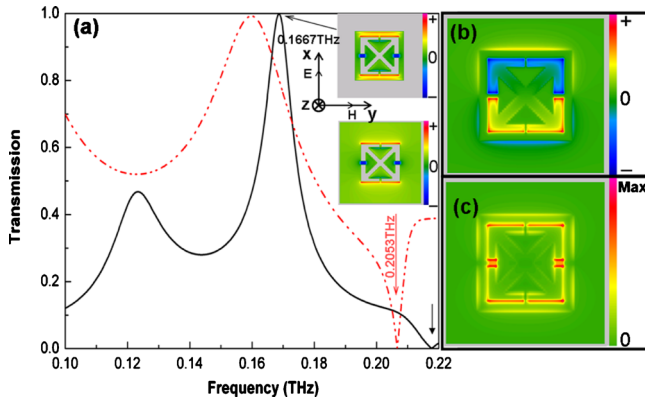


FIG. 2. (Color online) (a) Simulated transmission spectra for both the MM array (red dotted-dashed line) and hole array filled with MM patches (black curve). The insets show the field patterns of the x-component electric field at the peak frequency of the sample and that at dip frequency of MM array. Similarity of the simulated patterns supports the Fano resonance interpretation. (b) Simulated field pattern for the z-component electric field on metal-dielectric interface. (c) Simulated field pattern for the total electric field intensity on metal-dielectric interface, where great field enhancement in gaps is observed.

mission may be ascribed to the interaction between local resonance and continuum scattering channel, and it may be understood within Fano scattering framework, in which an asymmetric profile in the transmission spectrum can follow the profile¹⁴

$$f(\omega) = \frac{\left(q_F + \frac{\omega - \omega_r}{\Gamma/2}\right)^2}{1 + \left(\frac{\omega - \omega_r}{\Gamma/2}\right)^2}, \quad (1)$$

where $q_F = 2(\omega_r - \omega_0)/\Gamma$ is the Fano parameter describing the asymmetry of the transmission line shape, ω is frequency, ω_r is the resonant frequency of the bound state, ω_0 indicates the frequency at which the spectrum has a minimum, and Γ is the width of the narrow band.

Some qualitative deductions about the type of resonance and the sign of q_F may be obtained from the simulated spectra shown in Fig. 2. Due to the large spacing separation between the MM patches in the MM array, the resonance frequency of a MM patch (bound state), ω_r , can be identified to be that of MM array. The latter is given by the dip frequency in the transmission spectrum of the MM array (red dotted-dashed line). It can be observed from Fig. 2(a) that the dip frequency of the sample, ω_0 , is slightly higher than ω_r . Hence from the definition of q_F , its value is negative here. As the peak transmission frequency of a Fano profile is given by $\omega_{\text{peak}} = \omega_r + (\Gamma/2q_F)$, it follows that $\omega_{\text{peak}} < \omega_r < \omega_0$.

We have carried out Fano fitting for both the experiment and simulation spectra, in which the transmission spectrum of the metal hole array characterizes the nonscattering continuum channel. The Fano function $f(\omega)$ is obtained by normalizing the transmission spectrum to the transmission through the nonscattering channel.¹⁹ The fitted Fano parameter from the experimental data is ~ -5 , whereas the fitted Fano parameter from simulation is ~ -6 , consistent with our qualitative analysis. The fitting also reveals the transmission peak frequency of 0.17 THz for the simulation, and for the experiment it is 0.165 THz. The bandwidth obtained by fitting simulation data ($\Gamma = 0.015$ THz) is about two times of

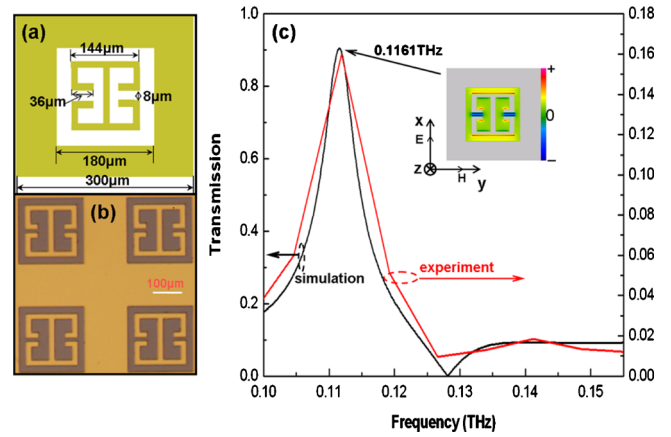


FIG. 3. (Color online) (a) Schematic illustration of second sample's microgeometry that shows the dimensions of the metamaterial patches in the hole array. (b) An optical image of the sample. (c) Simulated and measured transmission spectrum of the sample with the incident field of x-polarization. The inset shows the field pattern for the (x-component) electric field.

that obtained by fitting experiment data ($\Gamma = 0.008$ THz). Also the fitted transmission minimal frequency from simulation is $\omega_0 = 0.217$ THz, whereas that from experiment data is $\omega_0 = 0.184$ THz. Thus good agreement is obtained as seen by comparing these fitting parameters with those shown in measured [Fig. 1(c)] and simulated [Fig. 2(a)] spectra.

Simulated field distributions of the x-component electric field, for both the sample (at its peak frequency) and the MM array (at its dip frequency), are shown in the insets of Fig. 2(a). It is obvious that the field distributions around the MM patches are very similar. This similarity essentially clarifies the origin of the transmission peak to be the local MM patch resonance and supports Fano resonance interpretation above. The field pattern for the z-component of the electric field (perpendicular to the metal surface) on the metal-dielectric interface is shown in Fig. 2(b). In contrast with the conventional ET, there are no surface propagating modes but only local modes. In Fig. 2(c), the simulated total electric field on the metal-dielectric interface is shown. The field in the gap space is seen to be significantly enhanced and up to five times higher in intensity than that of metal hole array at its peak frequency.

The transmission characteristics of the sample are controlled by the resonance mode(s) of MM patches. To demonstrate, we have fabricated and tested another anisotropic MM structure. In Fig. 3(a) the sample configuration is shown and Fig. 3(b) shows an image of the actual sample. Measured and simulated transmission spectra are presented by the red and black curves in Fig. 3(c), showing good agreement in both the peak and dip frequency positions. Again, the field in the gap space is seen to be enhanced significantly (inset). Under the situation of our current sample and incident polarization, the wavelength of transmission peak frequency is over 15 times the size of the hole, even more subwavelength than the fractal aperture array.²⁰

For the same sample shown in Fig. 3, when the polarization changes from the x direction to the y direction, the anisotropy of the sample causes the resonant frequency of Fano bound state locating much closer to the FP peak frequency at 0.195 THz. Owing to this difference, the transmission profile is no longer a single peak but a double peak

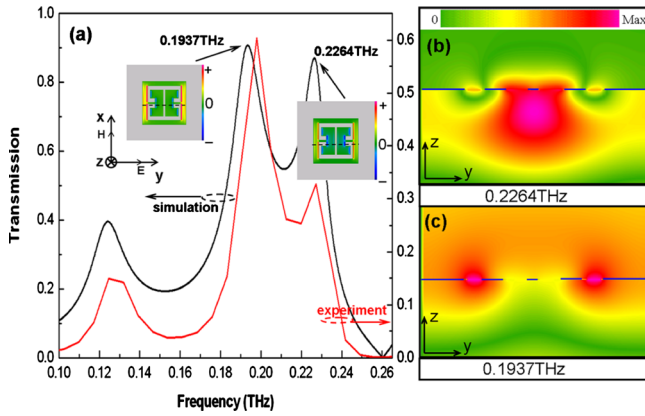


FIG. 4. (Color online) (a) Simulated and measured transmission spectra with the incident field of y -polarization. The insets show that field patterns of y -component electric field at the two resonant transmission peaks. (b) Field pattern on y - z plane [corresponding to the cut along the black dashed line in the insets shown in (a)] for the total magnetic field intensity at the higher resonant transmission frequency. (c) Field pattern on the y - z plane [on the same y - z plane cut as that for (b)] for the total magnetic field intensity at the lower resonant transmission frequency. In (b) and (c) the silicon substrate is at the bottom of the figure. The blue lines indicate the metallic layer.

profile, where the lower frequency peak represents a hybridized mode between the Fano resonance and the FP resonance. The simulation results [black curve in Fig. 4(a)] show good agreement with the experiment [red curve in Fig. 4(a)]. The magnetic field patterns simulated at the resonant frequencies, shown in Figs. 4(b) and 4(c), also lend support to the hybridization picture. At 0.226 THz, which is close to resonant frequency of the bare MM patches, the magnetic field intensity is enhanced in the inner gaps of MM [Fig. 4(b)]; at the lower transmission peak frequency, 0.194 THz, the field enhancement occurs at the gap between the MM patch and the edges of the hole. The latter is consistent with the physical picture of the field being squeezed by the edge of the metal hole and the MM patch with the microgeometry of the MM patch not playing much role. Hence the upper transmission peak frequency has the MM local resonance characteristic, the lower transmission peak frequency has more of the FP characteristic.

W.W. and P.S. wish to acknowledge the support for

this work by NSFC/RGC Joint Research Grant No. N_HKUST632/07 and RGC Grant No. HKUST 3/06C. M.T. and F.M. would like to thank the support from the Ministry of Education, Science, Sports and Culture of Japan under the Grant-in-Aid for Scientific Research (A) No. 20244047 and for Young Scientists (B) No. 21760036.

- ¹T. W. Ebbesen, H. J. Lezec, H. F. Ghaemi, T. Thio, and P. A. Wolff, *Nature (London)* **391**, 667 (1998).
- ²F. J. García de Abajo, *Rev. Mod. Phys.* **79**, 1267 (2007).
- ³M. Liscidini and J. E. Sipe, *Appl. Phys. Lett.* **91**, 253125 (2007).
- ⁴Z. Ruan and M. Qiu, *Phys. Rev. Lett.* **96**, 233901 (2006).
- ⁵W. Zhang, A. K. Azad, J. Han, J. Xu, J. Chen, and X. C. Zhang, *Phys. Rev. Lett.* **98**, 183901 (2007).
- ⁶F. J. García-Vidal, L. Martín-Moreno, H. J. Lezec, and T. W. Ebbesen, *Appl. Phys. Lett.* **83**, 4500 (2003).
- ⁷H. J. Lezec, A. Degiron, E. Devaux, R. A. Linke, L. Martín-Moreno, F. J. García-Vidal, and T. W. Ebbesen, *Science* **297**, 820 (2002).
- ⁸Y. Alaverdyan, B. Sepúlveda, L. Eurenus, E. Olsson, and M. Käll, *Nat. Phys.* **3**, 884 (2007).
- ⁹F. Miyamaru, Y. Sasagawa, and M. W. Takeda, *Appl. Phys. Lett.* **96**, 021106 (2010).
- ¹⁰B. Brian, B. Sepúlveda, Y. Alaverdyan, L. M. Lechuga, and M. Käll, *Opt. Express* **17**, 2015 (2009).
- ¹¹A. H. J. Yang, S. D. Moore, B. S. Schmidt, M. Klug, M. Lipson, and D. Erickson, *Nature (London)* **457**, 71 (2009).
- ¹²W. J. Padilla, M. T. Aronsson, C. Highstrete, M. Lee, A. J. Taylor, and R. D. Averitt, *Phys. Rev. B* **75**, 041102(R) (2007).
- ¹³U. Fano, *Phys. Rev.* **124**, 1866 (1961).
- ¹⁴A. E. Miroshnichenko, S. Flach, and Y. S. Kivshar, *Rev. Mod. Phys.* **82**, 2257 (2010).
- ¹⁵B. Luk'yanchuk, N. I. Zheludev, S. A. Maier, N. J. Halas, P. Nordlander, H. Giessen, and C. T. Chong, *Nature Mater.* **9**, 707 (2010).
- ¹⁶B. Hou, J. Mei, M. Ke, W. Wen, Z. Liu, J. Shi, and P. Sheng, *Phys. Rev. B* **76**, 054303 (2007); It should be noted that from the thickness (500 μm) of the silicon substrate and its dielectric constant (12), the calculated FP peaks are at 0.09, 0.173, and 0.26 THz, with dips at 0.13 and 0.22 THz. The addition of MM array on the substrate will not significantly change the peak and dip frequencies. However, the addition of a metal hole array will essentially modify the impedance condition at one end of the FP resonant structure, with the effect of introducing a π phase shift. Hence the observed FP peaks should be at 0.13 and 0.21–0.22 THz, and the dips at around 0.09, 0.16–0.17, and 0.25 THz.
- ¹⁷X. Xiao, J. Wu, F. Miyamaru, M. Zhang, M. Takeda, C. Qiu, W. Wen, and P. Sheng, *Opt. Express* **18**, 18558 (2010).
- ¹⁸Simulations were performed using the software CONCERTO 6.5, Vector Fields Limited, England, 2007.
- ¹⁹A. Bärnthaler, S. Rotter, F. Libisch, J. Burgdorfer, S. Gehler, U. Kuhl, and H.-J. Stockmann, *Phys. Rev. Lett.* **105**, 056801 (2010).
- ²⁰B. Hou, X. Liao, and K. S. J. Poon, *Opt. Express* **18**, 3946 (2010).